

# FIELD EMISSION FROM A THERMALLY OXIDIZED Nb SAMPLE

S. Lagotzky\*, G. Müller, University of Wuppertal, D-42097 Wuppertal, Germany

## Abstract

The activation of enhanced field emission (EFE) on Nb is strongly influenced by the thickness  $d_{ox}$  of the surface oxide. EFE measurements on a single crystal Nb sample with an increased  $d_{ox}$  of about 100 nm after thermal oxidation (TO) revealed first EFE at 100 (150) MV/m and emitter number densities  $N$  up to 30 (40)  $\text{cm}^{-2}$  at 225 MV/m after cleaning with ionized  $\text{N}_2$  (dry ice cleaning, DIC). These results mean an improvement compared to wet anodized Nb. Moreover, TO is able to reduce  $N$  at the intended electric peak field of future accelerating structures for the International Linear Collider (ILC) by a factor 20 compared to the actually used Nb after DIC. The remaining EFE was mainly caused by surface defects and partially molten features with onset fields above 90 MV/m. Removal of the oxide by a heat treatment under ultra-high vacuum activated additional emitters and confirmed the suppression of EFE by the Nb oxide.

## INTRODUCTION

Enhanced field emission (EFE) from particulates and surface defects is one of the main field limitations of superconducting Nb cavities required for the International Linear Collider (ILC) [1]. The activation field  $E_{act}$  of such emitters and the emitter number density  $N$  is strongly influenced by the thickness  $d_{ox}$  of the Nb oxide layer. Removal of the native oxide layer ( $d_{ox} = 5$  nm [2]), e.g. by heat treatments (HT) under UHV up to 800°C, increases  $N$  significantly for  $E_{act}$  up to 160 MV/m with onset fields  $E_{on}$  down to 40 MV/m [3, 4]. Former EFE measurements on electrochemically oxidized Nb samples yielded for increasing  $d_{ox}$  between 53 and 463 nm a reduction of  $N$  from 18 to 2  $\text{cm}^{-2}$  at an  $E_{act}$  of 95 MV/m [5]. Similarly oxidized cavities proved that their quality factor is not affected by oxide layers up to 100 nm [6–8].

In order to improve the EFE performance of Nb surfaces with respect to ILC requirements (electric peak fields of 70 MV/m), we report here on a combination of Nb oxidation with advanced surface cleaning techniques. Single crystal Nb was used to avoid any grain boundary effects. Thermal oxidation (TO) in air was applied to receive a homogeneous layer with  $d_{ox}$  of about 100 nm. Such a TO should also be applicable for cavities. Systematic EFE measurements by means of a field emission scanning microscope (FESM) and a scanning electron microscope (SEM) on the same sample were performed both after TO with  $\text{N}_2$ -cleaning or dry ice cleaning (DIC) [9]. Supplementary measurements after removal of the oxide in both cases by a heat treatment (HT) under ultra-high vacuum (UHV) were carried out to prove the EFE suppression by the Nb oxide.

\*s.lagotzky@uni-wuppertal.de

## EXPERIMENTAL DETAILS

### Samples

We have used single crystal Nb discs ( $\varnothing=28$  mm) with an RRR of 250 welded to a Nb support rod. Such samples were polished in two steps: 1. buffered chemical polishing (BCP, HF (48%):  $\text{HNO}_3$  (65%):  $\text{H}_3\text{PO}_4$  (85%), 1:1:2) of 40  $\mu\text{m}$  and 2. electropolishing (EP, HF (40%):  $\text{H}_2\text{SO}_4$  (98%) 1:9) of 140  $\mu\text{m}$ . The resulting linear (square) roughness was about 80 nm (100 nm) as measured by means of optical profilometry [4]. Each sample has two marks on the edge for repositioning in different measurement systems with an accuracy of about 500  $\mu\text{m}$ .

At first, wet anodizing in  $\text{H}_2\text{SO}_4$  (10%) with a voltage of 25 V and a Nb sheet ( $\sim 50$   $\text{cm}^2$ ) as counter electrode in a distance of about 8 cm was tried on  $\text{N}_2$ -cleaned sample at room temperature. The resulting colour of the anodized surfaces was dark blue, but rather inhomogeneous. SEM analysis of the surfaces revealed many round features of about 10  $\mu\text{m}$  in size on the initially flat surface. Therefore, the wet oxidation was replaced by a TO within a muffle furnace. Heating at 360 °C for 40 min in air and subsequent natural cool-down resulted in a rather homogenous yellow colour (Fig. 1a) that correspond to an oxide thickness of about 100 nm.

Before and after TO the sample was cleaned with ionized and filtered  $\text{N}_2$  (*Simco-Ion Top Gun*, filter size 10 nm) at a pressure of 5 bar and immediately installed into the FESM. After the initial EFE measurements the oxide was removed in a resistive furnace inside the load-lock of the FESM (see Fig. 2) under UHV conditions ( $<10^{-4}$  Pa). The HT cycle consisted of a warm-up ramp (6.3 °C/min) from room temperature, the annealing at 400°C for 2 h and a natural cool-down phase (3 h). The temperature was controlled with a thermocouple (Pt10Rh-Pt type S) and regulated by a commercial PID-controller (JUMO cTRON 04) within  $\pm 1^\circ\text{C}$ . After this HT, the sample showed its initial metallic appearance.

For comparison, DIC (*CryoSnow* SJ-10) in a clean room (ISO 2) instead of the  $\text{N}_2$ -cleaning was applied before and after the TO. In order to avoid particulate contamination the sample was protected by an Al cap, as shown in Fig. 1b. This cap was also cleaned by DIC and not removed until the sample faced UHV conditions.

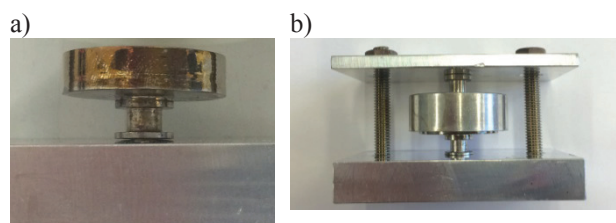


Figure 1: Colour of Nb sample after TO (a) and fixation of Al protection cap for the second TO step after DIC (b).

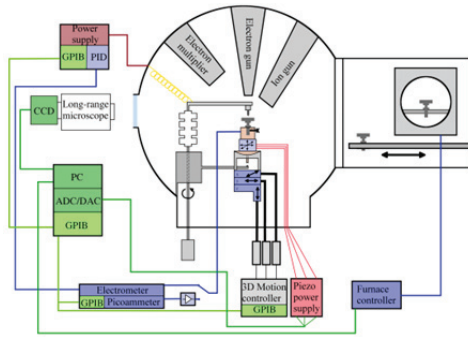


Figure 2: Schematic view of the FESM.

### Measurement Techniques

For the systematic EFE measurements we have used the non-commercial UHV-FESM ( $10^{-7}$  Pa) [10], which is shown schematically in Fig. 1. The sample was always investigated in the same area of  $10 \times 10$  mm<sup>2</sup>. In order to achieve a constant gap  $\Delta z$ , the surface tilt was corrected within  $\pm 2$   $\mu$ m relative to the truncated-cone W anode ( $\varnothing = 300$   $\mu$ m). The FESM employs a PID-regulated power supply (FUG HCN100M-10000, 10 kV, 10 mA) controlled by the EFE current as measured with an analog electrometer (Keithley 610C). Non-destructive voltage scans  $V(x,y)$  for a limited EFE current ( $I_{FE}$  up to 1 nA) were performed with a resolution of 150  $\mu$ m to localize emitters and to determine the emitter number density  $N$  as function of the applied activation field  $E_{act}$  in reasonable steps ( $\Delta V$  of 1 kV). Using the average  $\Delta z$  of 40  $\mu$ m estimated from a long range optical microscope image, electric field maps ( $E(x,y) = V(x,y)/\Delta z$ ) up to 225 MV/m were derived. Due to a slight tilting of the anode (e.g. in the holder or because of manufacturing), the determined values for  $E_{act}$  may have an error of up to 30%, although in the most cases the error is much lower.

For most of the strong emitters,  $I(V)$  characteristics were individually measured up to  $I_{FE}$  of 1 nA with a digital picoammeter (Keithley 6485). The actual  $\Delta z$  and thus the local field  $E$  were calibrated for each emitter from a PID-regulated  $V(z)$  plot for  $I_{FE}$  of 1 nA, which also yields the corresponding onset field  $E_{on}$ . Using the modified Fowler-Nordheim law [11]

$$I_{FE} = A \frac{S\beta^2 E^2}{\phi t^2(y)} \exp\left(-B \frac{\phi^{3/2} v(y)}{\beta_{FN} E}\right) \quad (1)$$

the field enhancement factor  $\beta$  and the emitting area  $S$  were derived for a given work function  $\phi$ . For simplicity, we have taken  $\phi = 4$  eV,  $v(y) = t(y) = 1$ ,  $A = 154$  and  $B = 6830$  for  $E$  in MV/m and  $I_{FE}$  in A. Finally, the emission sites were investigated with an SEM (JEOL JSM-6510) to search for the EFE origin.

## RESULTS AND DISCUSSION

### EFE Statistics

The first emitter on the N<sub>2</sub>-cleaned TO surface was activated at 100 MV/m. No additional activation was observed up to 150 MV/m (Fig. 3a). Five new emitting sites occurred at 175 MV/m (Fig. 3b), and increasing the field up to 225 MV/m resulted in 30 emitters (Fig. 3c). Similar results were obtained after DIC: the first stable emitter was activated at 150 MV/m (Fig. 3d), and 6 (40) spots were observed now at 175 MV/m (225 MV/m) as shown in Fig. 3e (Fig. 3f). Hence, N<sub>2</sub>-cleaning seems to be sufficient to suppress EFE up to 225 MV/m for single crystal Nb. Although the same area of the sample was investigated, it is remarkable that after the second TO many new emission sites at the same field levels as before can be found, while some others disappeared. Therefore, the activation of different emission sites hints for a slightly different oxidation process of the emitters.

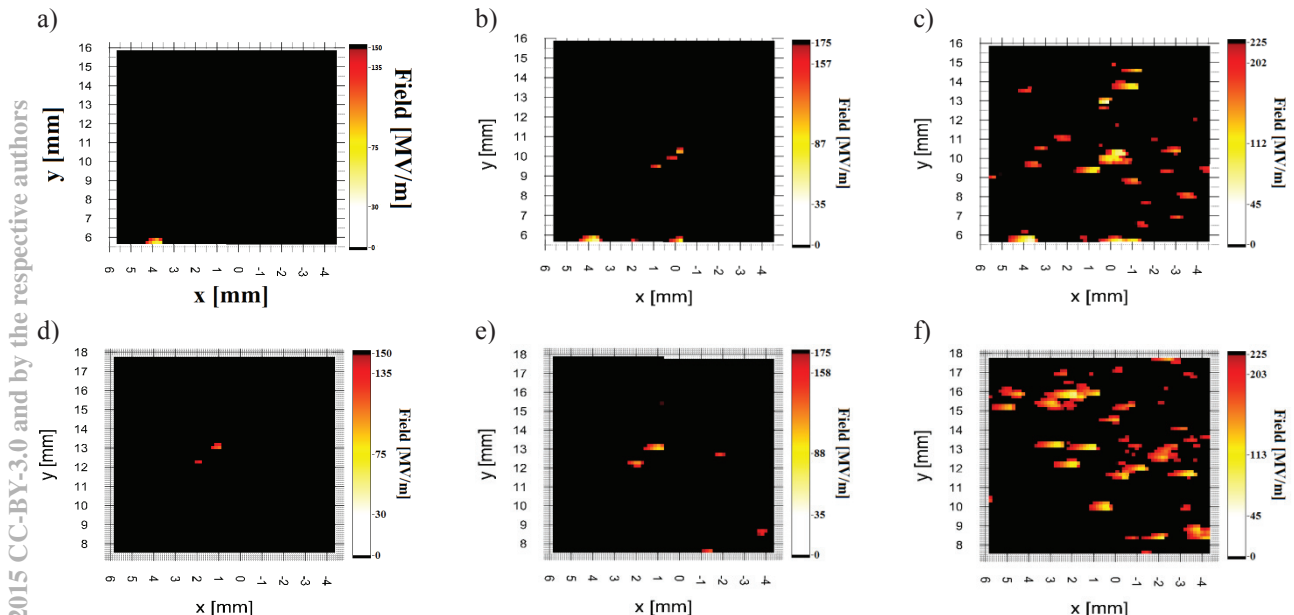


Figure 3: Field maps of thermally oxidized single crystal Nb after N<sub>2</sub>-cleaning (a-c) and DIC (d-f) at  $E_{act} = 150$  MV/m (a, d),  $E_{act} = 175$  MV/m (b, e) and  $E_{act} = 225$  MV/m (c, f).

In Fig. 4 the resulting  $N(E_{act})$  of the TO surface for both cleaning techniques are plotted in accordance to the statistical model for the activation of emitters on metallic surfaces [12]

$$N(E_{act}) = N_{tot} \cdot \exp(c_s) \cdot \exp\left(-c_s \cdot \frac{E_{lim}}{E_{act}}\right), \quad (2)$$

which depends on the total number of potential emitters  $N_{tot}$ , the field strength of the native insulating oxide  $E_{lim}$  and a surface condition parameter  $c_s$ . Obviously, the obtained results are independent of the cleaning technique within the statistical errors despite of the partially different emission sites. The linear least-square fit of the data result a slope  $B$  of  $-423.19 \pm 94.26$  ( $-465.32 \pm 93.63$ ) and  $y$ -intercept  $A$  of  $3.17 \pm 0.57$  ( $3.54 \pm 0.52$ ) for the  $N_2$ -cleaned (DIC) surface. The correlation coefficient was rather high ( $> 0.93$ ) in both cases. It is remarkable that the TO of Nb leads to an increased slope in comparison to EP/BCP Nb after DIC with a native oxide layer, which yields in  $B = -276.45$  and  $A = 2.12$  [12]. This EFE performance is a significant improvement compared to that of wet oxidized Nb surfaces [5]. Accordingly, TO leads to a much lower  $N$  compared to naturally oxidized Nb at  $E_{act}$  up to 125 MV/m, e.g. reduces  $N$  at the intended  $E_{peak}$  of the ILC from  $1.5 \times 10^{-2} \text{ cm}^{-2}$  to  $7.8 \times 10^{-4} \text{ cm}^{-2}$ .

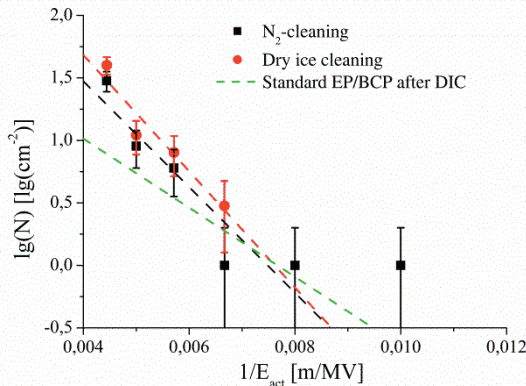


Figure 4: Dependence of the emitter number density from the activation field of TO Nb after  $N_2$ -cleaning and DIC plotted in accordance to eq. (2). The dashed lines are least-square fits and compared to the result for EP/BCP Nb after DIC [12].

The EFE measurements were repeated after removal of the oxide for both cleaning techniques. As expected, the EFE of the  $N_2$ -cleaned (DIC) sample started already at much lower  $E_{act}$  of 75 MV/m (100 MV/m), and many additional emitters were observed at higher fields. The resulting  $N$  at 225 MV/m was increased to  $60 \pm 8 \text{ cm}^{-2}$  ( $65 \pm 8 \text{ cm}^{-2}$ ) on the  $N_2$ -cleaned (DIC) surface as shown in Fig. 5. Most emitters, which were already activated on the TO surface, reappeared after the HT400, but few emitters disappeared up to 225 MV/m. This suggests a significant role of conducting channels for the EFE, which are usually formed in the oxide during the

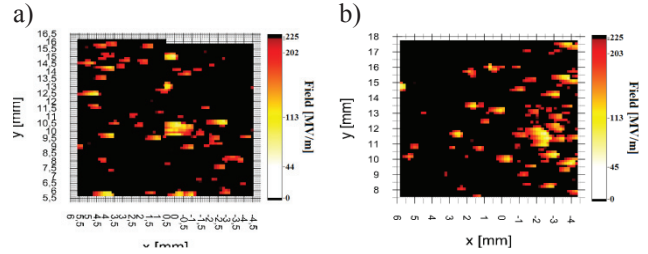


Figure 5: Field maps of the same sample as in Fig. 3 after oxide removal in case of  $N_2$ -cleaning (a) and DIC (b).

activation[13]. Removal of this channel together by the HT changes  $\beta$  [12].

### Single Properties

Guided by the field maps, local EFE measurements and SEM analysis were performed for 9 (10) strong emitters activated on the oxidized surface after  $N_2$ -cleaning (DIC). As expected, the EFE on both surfaces was dominated by surface defects, e.g. scratches, and only one foreign particulate was found on the  $N_2$ -cleaned surface. Fig. 6a shows a typical example for a small surface defect located on a long scratch. The  $I(I)$  dependence of the corresponding emitter on the TO surface resulted in fluctuating FN-parameters ( $\beta = 22-53$ ,  $S \sim 10^4-10^4 \mu\text{m}^2$ ) and low  $E_{on} = 95 \text{ MV/m}$  (Fig. 6b). After oxide removal, the EFE became more stable (Fig. 6c,  $\beta = 35$ ,  $S \sim 2 \times 10^5 \mu\text{m}^2$ ,  $E_{on} = 165 \text{ MV/m}$ ). Moreover, some large

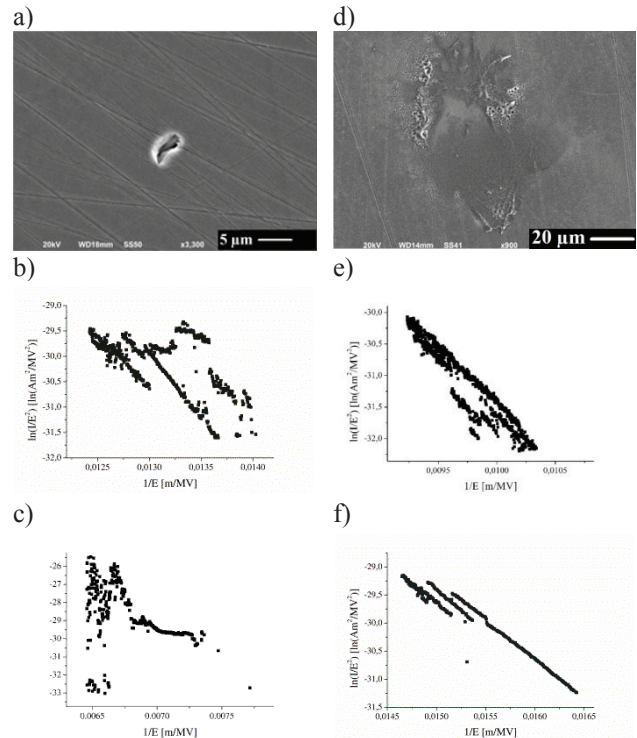
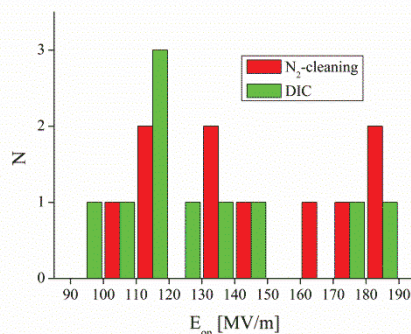


Figure 6: REM images (a, d) and FN-Plots before (b, e) and after (c, f) removal of oxide of a typical surface defect (a-c) and a partially molten emission site (c-f).

features with starburst-like halos due to  $\mu$ -discharges [14] were found at the emission sites as shown in Fig. 6d. The corresponding emitter provided much more stable  $I(V)$  curves, and the FN plots yielded  $\beta = 21$ -30,  $S \sim 10^3$ - $10^2 \mu\text{m}^2$  and  $E_{on} = 110$  MV/m for the TO surface (Fig. 6e) and  $\beta = 32$ -40,  $S \sim 10^2$ - $10^1 \mu\text{m}^2$  and  $E_{on} = 71$  MV/m (Fig. 6f) after HT. An influence of DIC on the surface roughness in the  $\mu\text{m}$ -scale was not observed. Comparing the EFE of both surface defects, HT leads to some EFE stabilization. The length of the conducting channels, however, is neither correlated to the FN parameters nor to the final  $E_{on}$  values in contrast to the  $E_{act}$  values.

The measured  $E_{on}$  values (Fig. 7a) as well as the  $\beta$  and  $S$  values (Fig. 7b) obtained for the oxidized surfaces are hardly influenced by the applied surface cleaning technique. This confirms that the EFE of TO Nb is caused by similar surface defects in both cases. It is remarkable that all onset fields are above 90 MV/m now, what is 20 MV/m higher than the intended electric peak field of future ILC accelerating structures. Furthermore, some  $S$ -values are significantly larger than the area of the used anode ( $\sim 7 \times 10^4 \mu\text{m}^2$ ). This hints for non-FN-like EFE from Nb surfaces independent of the oxide thickness [15].

a)



b)

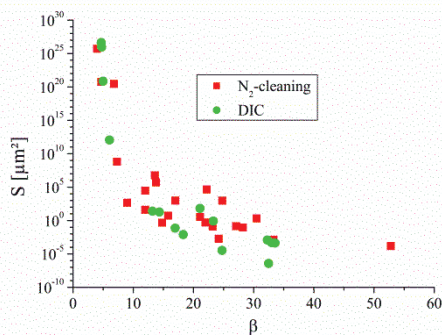


Figure 7: Histogram of  $E_{on}$  (a) and  $S$  vs.  $\beta$  dependence (b) of the measured emission sites on oxidized Nb after N<sub>2</sub>-cleaning and after DIC.

## CONCLUSIONS AND OUTLOOK

Thermal oxidation of single crystal Nb is able to suppress parasitic EFE and results in activation fields up to 150 MV/m. This result is independent of the applied cleaning technique (N<sub>2</sub>-cleaning or DIC). The remaining EFE is dominated by surface defects and partially molten features with starburst-like halos. The positive effect of the oxide layer on the EFE suppression is confirmed by comparison to results on the heated surface with much reduced oxide thickness. Therefore, TO is able to reduce the emitter number density at the intended  $E_{peak}$  of the future ILC accelerating structures significantly to  $8 \times 10^{-4} \text{cm}^{-2}$ , which is a factor  $\sim 20$  lower than our EFE result for the actually used Nb after DIC. It is remarkable that this EFE performance means a significant progress with respect to previous results of wet oxidized Nb surfaces.

As next step EFE measurements on polycrystalline Nb surfaces with different oxide thickness should be performed to clarify the discussed EFE activation and the relevance for future ILC cavities.

## ACKNOWLEDGMENT

This work was funded by BMBF project 05H12PX6.

## REFERENCES

- [1] H. Padamsee, *RF Superconductivity* (WILEY-VCH, Weinheim, 2009).
- [2] M. Grundner & J. Halbritter, *J. Appl. Phys.* **51**, 397 (1980).
- [3] A. Navitski, S. Lagotzky, et al., *Phys. Rev. Spec. Top. - Accel. Beams* **16**, 112001 (2013).
- [4] S. Lagotzky, G. Müller, et al., TUP093, Proc. SRF13, <http://jacow.org>
- [5] A. T. Wu, S. Jin, et al., MOPC118, Proc. IPAC11, <http://jacow.org>
- [6] H. Martens, H. Diepers, & R. K. Sun, *Phys. Lett. A* **34**, 439 (1971).
- [7] H. Pfister, *Cryogenics*. **16**, 17 (1976).
- [8] J. Sekutowicz, *ICFA Beam Dyn. Newsl.* **39**, 112 (2006).
- [9] A. Dangwal, G. Müller, et al., *J. Appl. Phys.* **102**, 044903 (2007).
- [10] D. Lysenkov, G. Müller, *Int. J. Nanotechnol.* **2**, 239 (2005).
- [11] R. G. Forbes, *J. Vac. Sci. Technol. B* **17**, 526 (1999).
- [12] S. Lagotzky, G. Müller, submitted to *Nucl. Instr. Methods Phys. Res. Sect. A* (2015).
- [13] R. V Latham, *High Voltage Vacuum Insulation* (Academic Press, London, 1995).
- [14] J. Knobloch, PhD thesis, Conell (1997).
- [15] J. Halbritter, *Surf. Sci.* **122**, 80 (1982).